Journal of Solid State Chemistry **152,** 526–532 (2000)
doi:10.1006/jssc.2000.8724, available online at http://www.idealibrary.com on IDEAL®

Synthesis and Properties of Spinel-Type Co–Cu–Mg–Zn–Cr Mixed Oxides

G. L. Castiglioni,* G. Minelli,† P. Porta,†,[1] and A. Vaccari‡

*Lonza SpA, Via Fermi 51, 24020 Scanzorosciate BG, Italy; †Centro del Consiglio Nazionale delle Ricerche su "Struttura e Attività Catalitica di Sistemi di Ossidi" (SACSO), c/o Dipartimento di Chimica, Università degli Studi di Roma "La Sapienza," Piazzale Aldo Moro 5, 00185 Roma, Italy; and ‡Dipartimento di Chimica Industriale e dei Materiali, Università degli Studi di Bologna, Viale del Risorgimento 4, 40136 Bologna, Italy

Received August 11, 1999; in revised form February 29, 2000; accepted March 27, 2000

Different mixed oxides containing Cu, Zn, Co, Mg, and Cr were obtained by calcining hydroxycarbonate precursors at different temperatures (653 or 873 K). Characterization was performed by X-ray diffraction, thermal analysis, infrared and reflectance spectroscopy, and BET surface area determination. Depending on metal composition the mixed oxides were constituted by CuO, ZnO, $CuCrO_4$ $ZnCr_2O_4$, $CoCr_2O_4$, and $Co_xCu_{1-x}Cr_2O_4$, $Mg_xCu_{1-x}Cr_2O_4$, $Co^{2+}Co^{3+}_xCr_{2-x}O_4$ solid solutions. The phase evolution during reduction of the mixed oxides, followed by *in situ* X-ray diffraction up to 973 K, showed that the reducible species, when present, were CuO, $CuCrO_4$, tetragonal $Co_xCu_{1-x}Cr_2O_4$ and $Mg_xCu_{1-x}Cr_2O_4$ spinels, with metallic copper and cubic spinels as final products of reduction. © 2000 Academic Press

1. INTRODUCTION

Reduced copper chromites containing or not other elements are widely employed as catalysts for many reactions, such as hydrogenation of organic compounds (1–9), alcohol decomposition or dehydrogenation (10, 11), ester hydrogenolysis (12), and, more recently, environmental applications (13–15). Cu–Zu–Cr(Al) mixed oxides have been also extensively studied as catalysts for methanol or higher alcohol synthesis from H_2 and CO (16–21). It has also been shown that addition of cobalt to $Cu/ZnO/M_2O_3$ catalysts tends to increase the selectivity in higher alcohols or hydrocarbons in comparison to that in methanol (22–26).

It has been reported that mixed catalysts are much more active than each of the components and that the activity is enhanced if great homogeneity of the oxides is achieved. Materials which satisfy such requirements are preferably derived by thermal decomposition of precursors containing all the metal cations in the same phase (26–30).

[1]To whom correspondence should be addressed.

The aim of this work was to synthesize high surface area (Cu, Co, Zn, Mg)–Cr mixed oxides, with different metal/Cr atomic ratios, obtained at relatively low temperature of calcination from hydroxycarbonate precursors, to determine some of their structural properties, and to investigate their reactivity to reduction.

2. EXPERIMENTAL PROCEDURES

Precursors were obtained by coprecipitation at $pH = 8.0 \pm 0.1$ pouring 0.5 liter of a 0.6 mol liter^{-1} solution of metal nitrates in suitable proportions to 1 liter of a 0.8 mol liter^{-1} $NaHCO_3$ solution at a constant temperature of 333 K and under vigorous stirring. The slurry was digested for 3 h under the same conditions. All precipitates were repeatedly washed with cold distilled water to eliminate the excess of Na^+ and NO_3^- ions. After washing, the sodium content was analyzed by atomic absorption and found to be less than 100 ppm. Once washed, the solids were heated in an oven at 363 K for 12 h and finely ground. The oxides were obtained by calcining the precursors for 14 h at 653 and 873 K.

Metal content was determined by atomic absorption with a Varian SpectrAA-30 instrument and found for all metals to agree within 5% with the nominal one.

X-ray diffraction (XRD) powder patterns were recorded using a Philips PW 1729 diffractometer equipped with an IBM PS2 computer for data acquisition and analysis (software APD-Philips) and a HP plotter. Scans were taken with a 2θ step size of 0.01° by using Ni-filtered Cu$K\alpha$ radiation. The phase evolution during the reduction process was studied by *in situ* XRD in an Anton-Paar HTK10 camera attached to a Philips diffractometer equipped with inner heating block-sample holder, and with variable temperature and feed controls. The samples calcined at 653 K were reduced step by step in the temperature range 373–973 K for 10 min at each step of 100 K in a flow of 45–50 ml min^{-1} of H_2/N_2 mixture (6/94 v/v). XRD patterns were recorded

0022-4596/00 $35.00
Copyright © 2000 by Academic Press
All rights of reproduction in any form reserved.

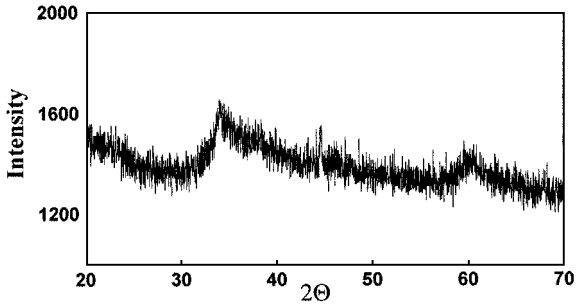

FIG. 1. X-ray diffraction pattern for the Cr/Cu/Mg = 50/40/10 precursor dried at 363 K

after each step of reduction in the range of $2\theta = 15$–50°, since this is the range in which the strongest X-ray reflections of the initial and most likely reduced phases present could occur. Lattice parameters of the spinel phases were calculated by means of the UNITCELL program.[2]

Reflectance spectra were recorded in the wavelength range 4,000–50,000 cm^{-1} with a Varian CARY 5E spectrometer equipped with an IBM SP2 computer for data acquisition and analysis (software Spectra Cal.-Galactic Industries Corp.), and using PTFE as reference.

IR spectra were recorded using the KBr disk technique and a Perkin–Elmer 1700 Fourier-transform (FTIR) spectrometer in the range 4000–400 cm^{-1} range.

BET surface areas were measured by N_2 adsorption using a Carlo Erba Sorpty 1750 apparatus.

Thermogravimetric analysis was performed using a Perkin–Elmer TGS-2 thermobalance, with an N_2 flow of 50 ml min^{-1} and a constant heating rate of 10 K min^{-1}

3. RESULTS AND DISCUSSION

3.1. Precursors

All dried precipitates showed XRD patterns typical of quasi-amorphous phases (see Fig. 1 as example). However, two broad bands at $d = 2.6$ Å ($2\theta \approx 35^\circ$) and 1.5 Å ($2\theta \approx 60^\circ$) are visible (except for the cobalt-containing materials), and they may be attributed to the hydrotalcite-type (HT) hydroxycarbonate (31–33). It must be noted that the synthesis of HT phases containing up to 50% of trivalent cations (as atomic ratio) have been already reported (34, 35).

The precipitates were identified as hydroxycarbonates on the basis of IR analysis (36). Note that identification by IR is not a diagnostic tool for HT compounds, but it is useful to check the anions in the interlayer between the brucite-like sheets (32). Independently from the chemical composition [the IR spectrum for Cr/Cu/Mg = 50/40/10 atomic composition is shown in Fig. 2a, as example], all samples present a large absorption band in the 400–600 cm^{-1} range,

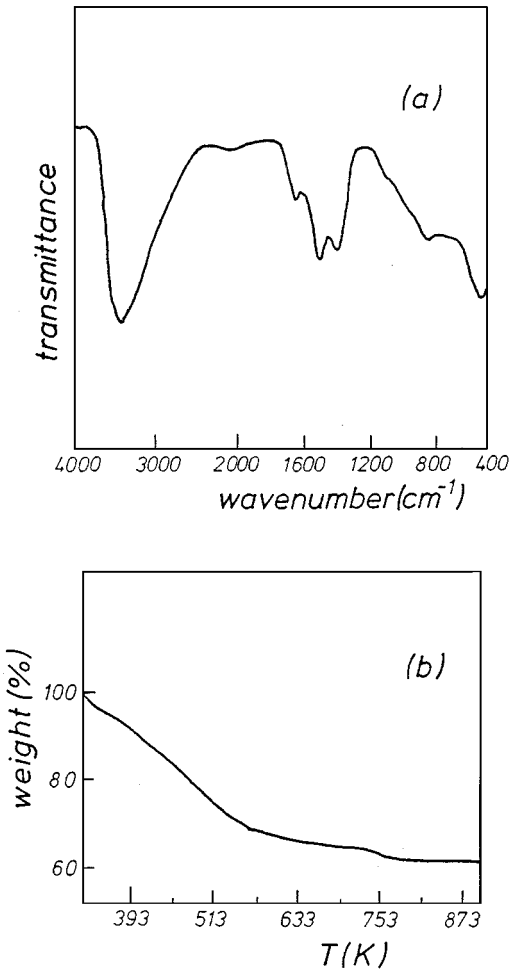

FIG. 2. (a) IR spectrum for the Cr/Cu/Mg = 50/40/10 precursor dried at 363 K. (b) Thermogram for the Cr/Cu/Mg = 50/40/10 precursor dried at 363 K.

attributable to an *M*–O vibration, whose intensity is related to the chromium content (37). It may thus be hypothesized the presence of a chromium hydroxide-type phase, also taking into account the occurrence of an absorption of less intensity at 830 cm^{-1}. The splitting of the ν_3 frequency of the carbonate ion with the appearance of two bands in the 1350–1500 cm^{-1} range (with a separation between the peaks of about 100 cm^{-1}, typical of basic salt) and the presence of a shoulder at about 1050 cm^{-1} are evidences of basic salt with a low degree of symmetry of the carbonate ions (36, 38, 39). Moreover, the intensity of the band at 1630 cm^{-1} is not only attributable to water deforming vibration but can be also due to the presence of bicarbonate ions (40, 41). Anyway, the low degree of symmetry of the carbonate anions and the presence of bicarbonate ions are not in contradiction between them and both the species may simultaneously coexist.

The thermograms performed in N_2 are similar for all precursors. Figure 2b shows, as an example, the thermal

[2] T. J. B. Holland and S. A. T. Redfern, *J. Appl. Crystallogr.* **30,** 84 (1997).

features for the sample Cr/Cu/Mg = 50/40/10 (atomic ratio %). The thermal patterns reveal a total weight loss which is in all cases in the 31–35% range, in agreement with the value calculated according to the decomposition of HT phases into mixed oxides, thus confirming their presence in the precipitates. The weight loss at higher temperatures may be ascribed, on the basis of the IR analysis, to the decomposition of residual carbonates and of small amounts of chromate formed in the previous step. As previously reported for Cu–Zn–Co–Cr–Al HT compounds (42–44), the thermal decomposition of the precipitates, independently of their relative metal content, occurs through the following steps: (i) at $T \leq 373$ K, loss of the residual water adsorbed on the surface of the sample; (ii) at $373 \leq T \leq 563$ K, loss of the crystallization water and dehydration of the brucite-like layers forming oxycarbonate species; (iii) at $563 \leq T \leq 743$ K, release of CO_2, leading to the formation of the mixed Me^{2+}–Me^{3+} oxides.

The reflectance spectra, although not diagnostic for the given HT precursor, are reported in Fig. 3 to show the octahedral (O_h) oxygen coordination around metals, coordination common for this type of compounds. All spectra are dominated by O_h–Cr^{3+}. Apart from the bands at lower energy (up to ca. 5000 cm^{-1}), due to surface water, the spectra of all the precipitates show the occurrence of two bands at ca. 17,500 and 24,500 cm^{-1} (specially evident in Fig. 3a, b, and d) which are due to the spin-allowed transitions of O_h–Cr^{3+} [45]. A shoulder at ca. 14,500 cm^{-1} corresponding to the spin-forbidden transition of O_h–Cr^{3+} is also visible. Note that the charge-transfer band, which starts at ca. 32,000 cm^{-1}, probably hides another spin-allowed transition of O_h–Cr^{3+}, expected at ca. 39,000 cm^{-1}. For the cobalt-containing samples (Fig. 3c and d) a band at ca. 8000 cm^{-1}, expected for Co^{2+} in octahedral symmetry (46) also appears. However, the expected strong band at ca. 20,000 cm^{-1}, observed in the O_h-$Co(H_2O)_6^{2+}$ complex, is not visible in the above spectra. When copper is present, the reflectance spectra (Fig. 3e and f show a broadening of the first band attributed to chromium; the left part of the large band occurs at ca. 12,500 cm^{-1} and corresponds to the expected transition for Cu^{2+} in a distorted octahedral coordination (45).

3.2. Oxides

XRD patterns of the precursors calcined at 653 K (Fig. 4) showed the prevailing presence of chromite spinels containing (depending on the divalent metal composition) Zn, Co, and Mg ions (Table 1). Moreover, samples of ZnO in Cr/Zn = 50/50 (Fig. 4b), CuO in Cr/Cu/Co = 50/40/10 (Fig. 4e) , and $CuCrO_4$, plus CuO in Cr/Cu/Mg = 50/40/10 (Fig. 4f) were revealed, in addition to the chromite spinel phase.

The precursors were also calcined at 873 K to increase their crystallinity and to allow a more accurate X-ray analysis of the phases present. The XRD powder patterns (Fig. 5) show the presence of cubic Zn- and Co-chromite spinels for the Cr/Zn and Cr/Co specimens, respectively, while for the Cr/Zn = 50/50 sample, the spinel phase plus ZnO can be observed. Table 1 reports the lattice parameters determined for the spinels present in the 873 K samples.

Cubic $ZnCr_2O_4$ in the Cr/Zn = 67/33 sample has a lattice parameter (a = 8.3438 Å) slightly higher than that quoted for this compound (8.3275 Å) in the literature. A similar a value (8.3433 Å) is found for the Cr/Zn = 50/50 sample, thus indicating that stoichiometric $ZnCr_2O_4$ also occurs in this material and that the excess of zinc is present as ZnO phase. For the stoichiometric Cr/Co = 67/33 material the lattice constant value of the spinel phase (8.3377 Å) is similar to that given for $CoCr_2O_4$ (8.330 Å) (31). On the other hand, the value of a = 8.2838 Å for the Co/Cr = 50/50 sample is

TABLE 1

Chemical and Structural Data for the Precipitates dried at 363 K and for the Samples Obtained by Heating the Precipitates at Different Temperatures and in Different Atmospheres

Composition[a]	T/K	Phases[b]	ϕ[c]	a[d]	c[d]
Cr/Zn = 67/33	363	Quasi-amorphous (H)			
	653	Spinel	80		
	873	c-$ZnCr_2O_4$	27	8.3438	
	H_2 (973 K)	c-$ZnCr_2O_4$			
Cr/Zn = 50/50	363	Quasi-amorphous (H)			
	653	Spinel + ZnO	119		
	873	c-$ZnCr_2O_4$ + ZnO	33	8.3433	
	H_2 (973 K)	c-$ZnCr_2O_4$ + ZnO			
Cr/Co = 67/33	363	Quasi-amorphous (H)			
	653	Spinel	59		
	873	c-$CoCr_2O_4$	n.d.	8.3377	
	H_2 (973 K)	c-$CoCr_2O_4$			
Cr/Co = 50/50	363	Quasi-amorphous (H)			
	653	Spinel	101		
	873	c-$Co^{2+}Co^{3+}_xCr_{2-x}O_4$	n.d.	8.2838	
	H_2 (973 K)	c-$Co^{2+}Co^{3+}_xCr_{2-x}O_4$			
Cr/Cu/Co = 50/40/10	363	Quasi-amorphous (H)			
	653	Spinel + CuO	120		
	873	t-$Co_xCu_{1-x}Cr_2O_4$ + CuO	38	6.0203[e]	7.9257[e]
	H_2 (673 K)	c-$CoCr_2O_4$ + Cu°			
Cr/Cu/Mg = 50/40/10	363	Quasi-amorphous (H)			
	653	Spinel + $CuCrO_4$ + CuO	70		
	873	t-$Mg_xCu_{1-x}Cr_2O_4$ + CuO	22	6.0232[e]	7.9093[e]
	H_2 (673 K)	c-$MgCr_2O_4$ + Cu°			

[a] Cr, Zn, Co, Cu, Mg atomic %.

[b] Phases detected by XRD for samples calcined at the given temperatures, and those observed at the end of the XRD *in situ* reduction (H_2/N_2) process performed on samples calcined at 653 K. H = hydroxycarbonate; c = cubic spinel; t = tetragonal spinel.

[c] Surface area ($m^2\ g^{-1}$).

[d] Lattice parameters (Å) relative to the spinel phase.

[e] Lattice parameters determined for the spinel phase after washing the samples with dilute and cold HCl (see text).

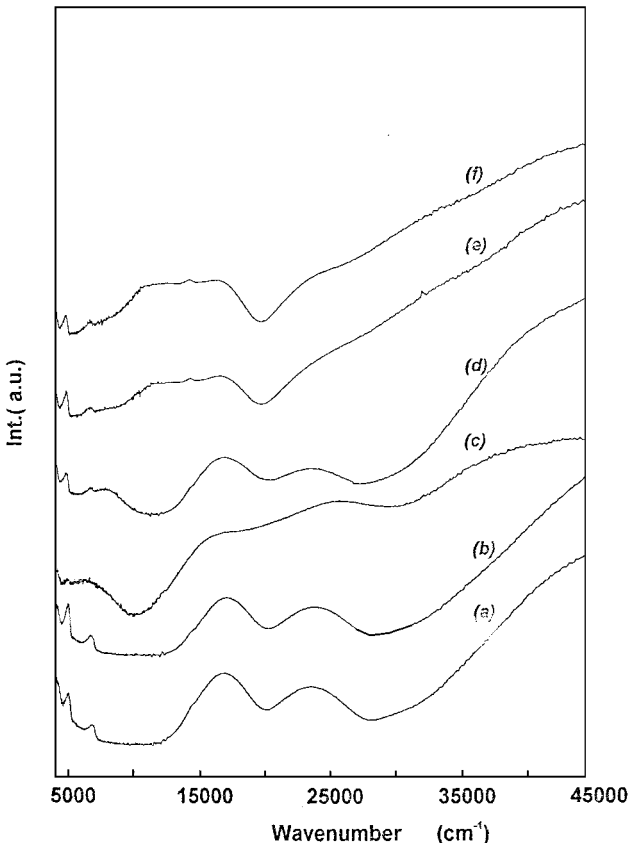

FIG. 3. Reflectance spectra for the precursors dried at 363 K with the following atomic compositions: (a) Cr/Zn = 67/33; (b) Cr/Zn = 50/50; (c) Cr/Co = 67/33; (d) Cr/Co = 50/50; (e) Cr/Cu/Co = 50/40/10; (f) Cr/Cu/Mg = 50/40/10.

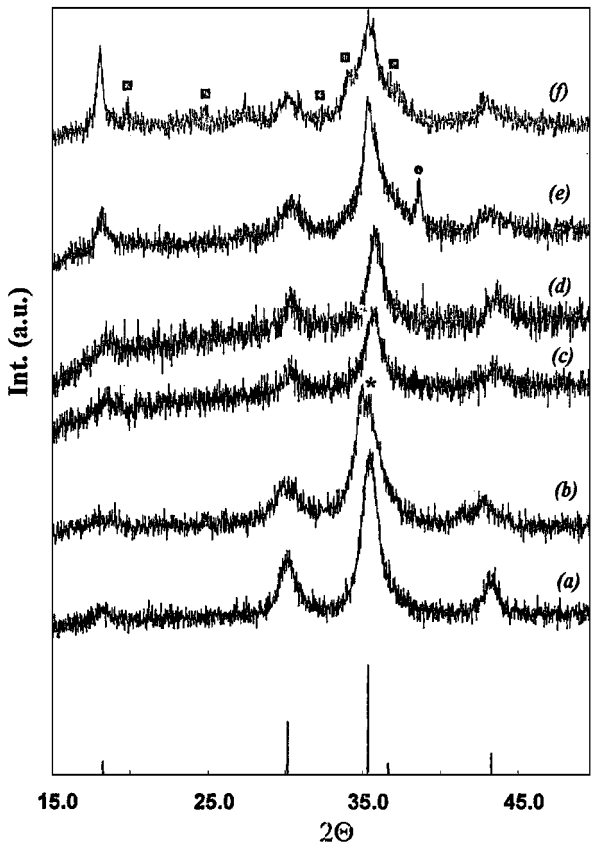

FIG. 4. X-ray diffraction patterns for the oxides obtained at 653 K: (a) Cr/Zn = 67/33; (b) Cr/Zn = 50/50; (c) Cr/Co = 67/33; (d) Cr/Co = 50/50; (e) Cr/Cu/Co = 50/40/10; (f) Cr/Cu/Mg = 50/40/10. Reference lines for the cubic chromite spinel are given at the bottom. Circle, asterisk, and square indicate the most intense X-ray lines for CuO, ZnO, and $CuCrO_4$, respectively.

lower and intermediate between those of $CoCr_2O_4$ (8.330 Å) and Co_3O_4 (8.084 Å) (31). It may be recalled that both $CoCr_2O_4$ and Co_3O_4 are isostructural, e.g., "normal" spinels with trivalent Cr^{3+} and Co^{3+} in the octahedral, and divalent Co^{2+} in the tetrahedral sites of the spinel lattice, so that the difference in the unit cell constant between $CoCr_2O_4$ and Co_3O_4 corresponds, at equal cation distribution, to the difference in size between Cr^{3+} and Co^{3+} [O_h ionic radii: $r^{3+}_{Cr} = 0.615$; $r^{3+}_{Co} = 0.545$ Å for Co^{3+} in low-spin configuration (47)]. The unit cell constant of the Co/Cr = 50/50 sample thus indicates that the spinel may be considered as a solid solution of $CoCr_2O_4$ and Co_3O_4, arising from an isomorphous Cr^{3+}/Co^{3+} cation substitution. On the basis of the lattice constant values for $CoCr_2O_4$ and Co_3O_4 end members and hypothesizing that the $Co^{2+}Co^{3+}_xCr^{3+}_{2-x}O_4$ spinel-type solid solution obeys Vegard's law (48), the $Co^{2+}Co^{3+}_{0.4}Cr^{3+}_{1.6}O_4$ composition can be suggested, in agreement with nominal cobalt and chromium content which should give the $Co^{2+}Co^{3+}_{0.5}Cr^{3+}_{1.5}O_4$ formula.

Figure 5e, and f shows that the spinel phases present in the ternary Cr/Cu/Co = 50/40/10 and Cr/Cu/Mg = 50/40/10 samples calcined at 873 K have a definite tetragonal lattice structure. Moreover, the formation of $Co_xCu_{1-x}Cr_2O_4$ and $Mg_xCu_{1-x}Cr_2O_4$ spinel solid solutions may be hypothesized also for the above compositions. For a better evaluation of the lattice parameters of the tetragonal spinel phase (without the interference of CuO) the Cr/Cu/Co = 50/40/10 and Cr/Cu/Mg = 50/40/10 specimens calcined at 873 K were washed with a cold and diluted HCl solution, removing completely CuO. The lattice parameters of the observed spinels are reported in Table 1. On the basis of both metal contents and observed phases, we suggest $Co_{0.4}Cu_{0.6}Cr_2O_4$ and $Mg_{0.4}Cu_{0.6}Cr_2O_4$ as the most probable formulae for the tetragonal (Co–Cu) and (Mg–Cu) chromite solid solutions, respectively.

It may be recalled that the XRD patterns of the samples calcined at 653 K (Fig. 4) revealed the presence of spinel and CuO in the Cr/Cu/Co = 50/40/10 material and spinel, CuO, and $CuCrO_4$ in the Cr/Cu/Mg = 50/40/10 sample. Due to the low resolution of the spectra, it was not possible to ascertain the structural symmetry, e.g., if cubic or

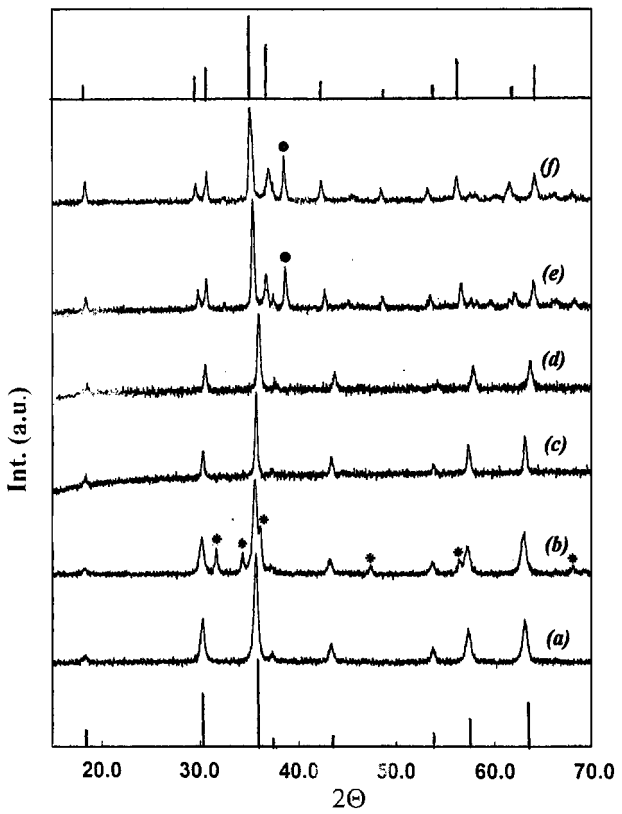

FIG. 5. X-ray diffraction patterns for the oxides obtained at 873 K: (a) Cr/Zn = 67/33; (b) Cr/Zn = 50/50; (c) Cr/Co = 67/33; (d) Cr/Co = 50/50; (e) Cr/Cu/Co = 50/40/10; (f) Cr/Cu/Mg = 50/40/10. Reference lines for the cubic and tetragonal copper chromite spinel are given at the bottom and at the top, respectively. Circle and asterisk indicate the most intense X-ray lines for CuO and ZnO respectively.

tetragonal, of the spinel phase. Moreover, the similarity of the lattice parameters for cubic $CuCr_2O_4$ (8.344 Å), $CoCr_2O_4$ (8.330 Å), and $MgCr_2O_4$ (8.333 Å) spinels (31) did not allow us to distinguish which spinel is formed at 653 K, i.e., if pure spinels or spinel solid solutions. However, we can suggest that, at the increase of the temperature from 653 to 873 K, a reaction occurs between the spinel phases (and $CuCrO_4$ copper chromate for the Cr/Cu/Mg = 50/40/10 sample), giving rise to tetragonal spinel solid solutions. Moreover, the similar values of tetrahedral ionic radii for Cu^{2+}, Co^{2+}, and Mg^{2+} [0.57, 0.58, and 0.57 Å, respectively, (47)] do not allow any direct confirmation on the solid solution formation. However, the difference between the evaluated unit cell volume for Cr/Cu/Co = 50/40/10 ($V = 287.26$ Å^3) and Cr/Cu/Mg = 50/40/10 ($V = 286.95$ Å^3), and that for tetragonal $CuCr_2O_4$ [$V = 283.31$ Å^3 (31)] tends to confirm the suggested formation of spinel solid solution for the above materials.

It is noteworthy that $CuCr_2O_4$, due to the Jahn–Teller effect, is one of the few $\frac{2}{3}$ spinels, which may crystallize other than in the cubic structure, in the more stable tetragonal form.

Note also, that in the Cr/Cu/Mg = 50/40/10 material calcined at 653 K a $CuCrO_4$ chromate phase was found in addition to $MgCr_2O_4$ and CuO (Fig. 4f). This agrees with the suggested mechanism of formation of spinel phases (especially for copper chromites) through chromate intermediate and its successive decomposition at higher temperature (49).

3.3. *Reducibility of the Oxides*

In situ reduction XRD analysis shows (Table 1) that the Cr/Zn = 67/33, Cr/Zn = 50/50, Cr/Co = 67/33, and Cr/Co = 50/50 samples obtained by calcining the precursors at 653 K are not reduced at all by a H_2/N_2 (6/94 v/v) mixture up to the final temperature of 973 K. Apart from a higher crystallinity, the original spinel phases (and ZnO for the Cr/Zn = 50/50 material) were detected at the end of the reduction experiment.

The following features regarding the reduction of the bulk structure emerged from the *in situ* XRD analysis performed on the Cr/Cu/Co = 50/40/10 sample: (i) at 473 K the pattern is the same as that taken at room temperature; (ii) at 523 K the disappearance of CuO, the decrease in intensity of the peaks belonging to the spinel phase and the first evidence of Cu° formation are detected; (iii) at $T > 523$ K more and more reduction is going on until 673 K, where the reduction is completed with formation of a high amount of metallic copper and a small amount of spinel phase. Figure 6 shows the comparison between the XRD patterns for the unreduced (a) and completely reduced (b) samples. Note that, in addition to the much lower intensity of the whole spectrum, the most intense spinel peak is shifted, in the reduced sample, toward higher 2θ angles. By taking into account that, as found in the most crystalline sample obtained at 873 K (Fig. 5), also the spinel present in the 653 K material is most likely a tetragonal $Co_xCu_{1-x}Cr_2O_4$ solid solution, and that the tetragonal $CuCr_2O_4$ and cubic $CoCr_2O_4$ spinels have their most intense peak at $2\theta = 35.2°$ and 35.7°, respectively (31), it could be inferred that starting from $T = 523$ K, in addition to the reduction of CuO, also the tetragonal $Co_xCu_{1-x}Cr_2O_4$ solid solution undergoes to reduction of copper (coming out the spinel lattice) giving rise to small amount of cubic $CoCr_2O_4$ and additional Cu°, with the excess of chromium probably present as not well crystallized spinel-like γ-Cr_2O_3 (not detected by XRD).

In situ reduction XRD analysis performed on the Cr/Cu/Mg = 50/40/10 sample has shown that up to 473 K the pattern is the same as that taken at room temperature. At 523 K, tenorite, CuO, and copper chromate, $CuCrO_4$, disappear with first evidence of metallic copper, whereas the spinel phase is still present. The end of the reduction, with a higher formation of metallic copper and evidence of a much smaller amount of the spinel phase, occurs at 673 K. Figure 7 shows the comparison between the XRD pattern of

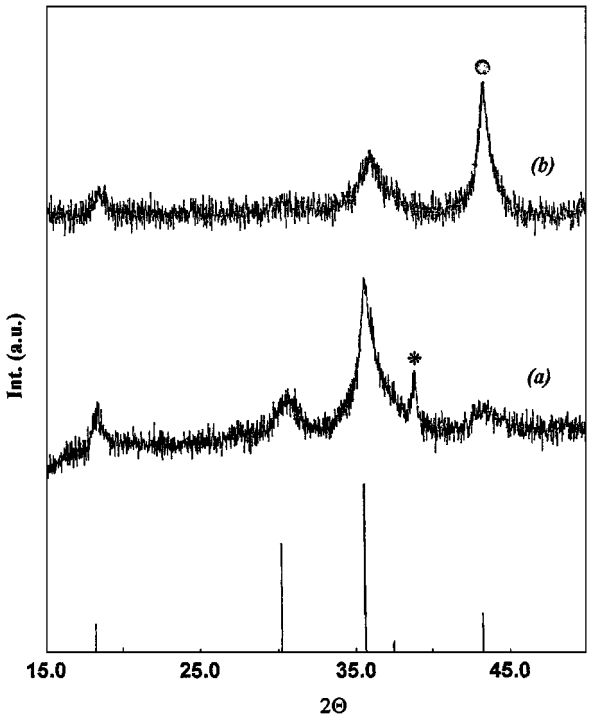

FIG. 6. X-ray diffraction patterns for the Cr/Cu/Co = 50/40/10 sample: (a) obtained by calcination of the precursor at 653 K, (b) subjected to *in situ* reduction (H_2/N_2 mixture = 6/94 v/v) at 673 K. At the bottom the X-ray lines of the reference cubic $CuCr_2O_4$ spinel are reported. Asterisk and circle indicate the most intense X-ray lines for CuO and Cu°, respectively.

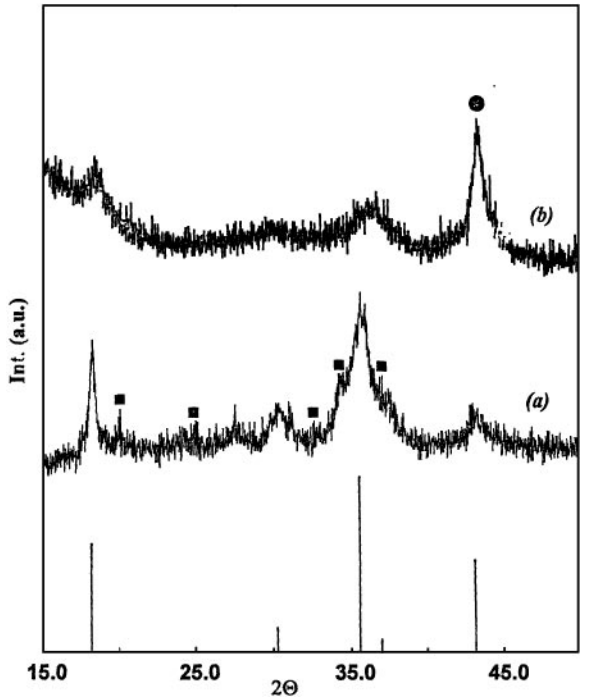

FIG. 7. X-ray diffraction patterns for the Cr/Cu/Mg = 50/40/10 sample: (a) obtained by calcination of the precursor at 653 K, (b) subjected to *in situ* reduction (H_2/N_2 mixture = 6/94 v/v) at 673 K. At the bottom the X-ray lines of the reference cubic $CuCr_2O_4$ spinel are reported. Square and circle indicate the most intense X-ray lines for $CuCr_2O_4$ and Cu°, respectively.

the unreduced sample (a) and that of the completely reduced one (b). Also in this case, in addition to the much lower intensity of the whole spectrum, the most intense spinel peak is shifted, in the reduced sample, toward higher 2θ angle. By considering that, as found in the more crystalline sample obtained at 873 K (Fig. 5), the spinel present in the 653 K material is also most likely a tetragonal $Mg_xCu_{1-x}Cr_2O_4$ solid solution, and that the tetragonal $CuCr_2O_4$ and cubic $MgCr_2O_4$ spinels have their most intense peak at $2\theta = 35.2^\circ$ and 35.7°, respectively (31), it might be inferred that, as previously discussed for the Cr/Cu/Co = 50/40/10 sample, at $T > 523$ also the copper ions inside the tetragonal $Mg_xCu_{1-x}Cr_2O_4$ solid solution undergo reduction with formation of additional Cu°, a small amount of cubic $MgCr_2O_4$, and not well-crystallized spinel-like γ-Cr_2O_3 phase, not detectable by XRD analysis.

4. CONCLUSIONS

By means of several complementary techniques the following points have been evidenced:

(i) Precursors are quasiamorphous hydroxycarbonate compounds, probably with a layered hydrotalcite-type structure.

(ii) Samples obtained by calcination of the precursors at 653 K, depending on the relative cation composition, consist of mixtures of chromite spinels, CuO, ZnO, and copper chromate.

(iii) Samples obtained by calcination of the precursors at 873 K, depending on the relative cation composition, consist of a mixture of ZnO and cubic spinels for the binary materials, and of a mixture of CuO and tetragonal spinel solid solutions for the ternary samples.

(iv) Under hydrogen treatment, the Cr/Zn and Cr/Co binary spinel phases are not reduced up to 973 K. For the ternary materials, in addition to the reduction of CuO and $CuCrO_4$, the tetragonal $Co_xCu_{1-x}Cr_2O_4$ and $Mg_xCu_{1-x}Cr_2O_4$ solid solutions transform to cubic $CoCr_2O_4$ and $MgCr_2O_4$ binary spinels, respectively, with formation of additional metallic copper.

ACKNOWLEDGMENTS

The authors thank Mr. M. Inversi for the useful assistance and technical support. The financial support from the Ministero Italiano per l'Università e la Ricerca Scientifica e Technologica (MURST, Rome) and from the Consiglio Nazionale delle Ricerche (CNR, Rome) are gratefully acknowledged.

REFERENCES

1. H. Adkins, *J. Am. Chem. Soc.* **72,** 2626 (1950).
2. S. Koritala, H. J. Dutton, *J. Am. Oil. Chem. Soc.* **43,** 556 (1996).
3. J. Jenck, J. E. Germain, *J. Catal.* **65,** 141 (1980).
4. G. L. Castiglioni, C. Fumagalli, R. Lancia, and A. Vaccari, *in* "Catalysis of Organic Reaction" (R. E. Malz, ed.), p. 65. Dekker, New York, 1996.
5. H. Zimmermann, T. Witzel, and E. Fuchs, German Pat. 19,518,018 (1996) to BASF A.G.
6. U. Herman, G. Emig, *Ind. Eng. Chem. Res.* **36,** 2885 (1997).
7. W. Kleemiss and M. Feld, Eur. Pat. Appl. 794,116 (1997) to Huels Aktiengesellschaft.
8. M. Takemoto, Y. Shima, and T. Abe, Eur. Pat. Appl. 773,215 (1997) to Mitsubishi Gas Chemical Co.
9. K. Turner, M. Sharif, J. Scarlet, and A. B. Carter, Eur. Pat. Appl. 301,853 (1998) to Davy McKee Ltd.
10. A. Iimura, Y. Inoue, and I. Yasumori, *Bull. Chem. Soc. Jpn.* **56,** 2203 (1983).
11. J. W. Evans, P. S. Casey, M. S. Wainwright, D. L. Trimm, and N. W. Cant, *Appl. Catal.* **7,** 31 (1983).
12. S. P. Tonner, D. L. Trimm, M. S. Wainwright, and N. W. Cant, *Ind. Eng. Chem. Prod. Res. Dev.* **23,** 384 (1984).
13. C. L. Honeybourne and K. R. Rasheed, *J. Mater. Chem.* **6,** 277 (1996).
14. A. Bhattacharyya and A. Basu, PCT9807652 (1998) to Amoco Co.
15. J. Abbasian and R. B. Slimane, *Ind. Eng. Chem. Res.* **37,** 2775 (1998).
16. K. Shimomura, K. Ogawa, M. Oba, and Y. Kotera, *J. Catal.* **52,** 191 (1978).
17. R. G. Herman, K. Klier, G. W. Simmons, B. P. Finn, J. B. Bulko, and T. P. Kobylinski, *J. Catal.* **56,** 407 (1979).
18. K. Klier, *Adv. Catal.* **31,** 243 (1982) and references therein.
19. Y. Okamoto, K. Fukino, T. Imanaka, and S. Teranishi, *J. Phys. Chem.* **87,** 3740 (1983).
20. G. Fornasari, S. Gusi, T. M. G. La Torretta, F. Trifirò, and A. Vaccari, *in* "Catalysis and Automotive Pollution Control" (A. Curcq and A. Frennet, eds.), p. 469 and references therein. Elsevier, Amsterdam, The Netherlands, 1987.
21. A. Sorbelli, F. Trifirò, and A Vaccari, *In* "Proc. IX Intern. Symp. Alcohol Fuels," p. 61. ECOFUEL, Milano, Italy, 1991.
22. P. Courty, G. Durand, E. Freund, and A. Sugier, *J. Mol. Catal.* **17,** 241 (1982).
23. G. Fornasari, S. Gusi, F. Trifirò, and A. Vaccari, *Ind. Eng Chem. Res.* **26,** 1501 (1987).
24. W. X. Pan, R. Cao, and G. L. Griffin, *J. Catal.* **114,** 447 (1988).
25. J. E. Baker, R. Burch, and S. E. Golunski, *Appl. Catal.* **53,** 279 (1989).
26. G. Fornasari, A. D'Huysser, L. Mintchev, F. Trifirò, and A. Vaccari, *J. Catal.* **135,** 386 (1992).
27. S. Gusi, F. Trifirò, A. Vaccari, and G. Del Piero, *J. Catal.* **94,** 120 (1985).
28. P. Porta, S. De Rossi, G. Ferraris, M. Lo Jacono, G. Minelli, and G. Moretti, *J. Catal.* **109,** 367 (1988).
29. G. Braca, A. M. Raspolli Galletti, F. Trifirò, and A. Vaccari, Italian Pat. 21,381 (1989) to C.N.R.
30. F. Trifirò, A. Vaccari, *in* "Structure–Activity and Selectivity Relationships in Heterogeneous Catalysis" (R. K. Grasselli and A. W. Sleight, eds.), p. 157. Elsevier, Amsterdam, The Netherlands, 1991.
31. International Center for Diffraction Data, JCPDS, Swarthmore, PA, 1991. Inorganic Powder Diffraction Files: $Cu_2Zn_4Al_2(OH)_{16}CO_3 \cdot 4H_2O$, 38-487; CuO, 5-661; Cu°, 4-836; $CuCr_2O_4$, cubic 26-509, tetragonal 34-424; $CuCrO_4$, 34-507; $ZnCr_2O_4$, 22-1107; $MgCr_2O_4$, 10-351; $CoCr_2O_4$, 22-1084; Co_3O_4, 9-418.
32. F. Cavani, F. Trifirò, and A. Vaccari, *Catal. Today* **11,** 173 (1991).
33. F. Trifirò, A Vaccari, *in* "Comprehensive Supramolecular Chemistry" (J. L. Atwood, D. D. McNicol, J. E. D. Davies, and F. Vögtle, eds.), Vol. 7, p. 251. Pergamon, Oxford, UK, 1995.
34. A. de Roy, C. Forano, K. El Malki, and J. P. Besse, *in* "Expanded Clays and Other Microporous Solids" (M. L. Occelli and H. E. Robson, eds.), Vol. 2, p. 108. Reinhold, New York, 1992.
35. F. Thevenot, R. Szymanski, and P. Chaumette, *Clays Clay Miner.* **37,** 396 (1989).
36. N. Nakamoto, *in* "Infrared and Raman Spectroscopy of Inorganic Compounds," 3rd ed., p. 243, Wiley, New York, 1978.
37. N. T. McDevitt and W. L. Baun, *Spectrochim.* Acta **20,** 799 (1964).
38. M. C. Gastuche, G. Brown, and M. M. Mortland, *Clays Clay Miner.* **7,** 177 (1967).
39. D. L. Bish and G. W. Brindley, *A. Mineral.* **62,** 458 (1977).
40. C. J. Serna, J. L. White, and S. L. Hem, *J. Pharm. Sci.* **67,** 324 (1978).
41. M. J. Hernandez-Moreno, M. A. Ulibarri, J. L. Rendon, and C. J. Serna, *Phys. Chem. Minerals* **12,** 34 (1985).
42. S. Morpurgo, M. Lo Jacono, and P. Porta, *J. Mater. Chem.* **4**(2), 197 (1994).
43. S. Morpurgo, M. Lo Jacono, and P. Porta, *J. Solid State Chem.* **119,** 246 (1995).
44. P. Porta, S. Morpurgo, and I. Pettiti, *J. Solid State Chem.* **121,** 372 (1996).
45. A. B. P. Lever, *in* "Inorganic Electron Spectroscopy" (A. B. P. Lever, Ed.), pp. 419, 557. Elsevier, Amsterdam, The Netherlands, 1984.
46. R. Pappalardo, D. L. Wood, and R. C. Linares, *J. Chem. Phys.* **35,** 2041 (1961).
47. R. D. Shannon, *Acta Crystallogr.* **A32,** 751 (1976).
48. A. R. West, *in* "Solid State Chemistry and its Applications," p. 366. Wiley, New York, 1987.
49. H. Charcosset, P. Turlier, and Y. Trambouse, *J. Chim. Phys.* **61,** 1257 (1964).